Proc. Indian Acad. Sci. (Chem. Sci.), Vol. 93, Number 1, January 1984, pp. 33–46.

A zero differential overlap study of chemical binding in ammonia-borane and carbonyl-borane

DULAL C GHOSH
Department of Chemistry, University of Kalyani, Kalyani 741 235, India

MS received 8 May 1982; revised 12 April 1983

Abstract. A CNDO/2*D* study of the charge distribution obtained through Mulliken population analysis in the ground state of the title compounds shows that the features of charge distribution found by several *ab initio* calculations are fairly well reproduced by this method. The one-particle density, the interference density at the mid-point of the bond axis and the kinetic part of the interference energy calculated through the deorthogonalized density matrices over a wide range of intermolecular separation between the donor and the acceptor show that the one-particle density and the interference density steadily grow with decreasing internuclear separation, while the kinetic interference energy starts with negative value at large distance, then decreases and passes through a minima near but above the equilibrium distance and then increases rapidly below it conforming to the characteristic general behaviour of the kinetic component of Morse curve. The orbital pairwise interference density and the corresponding kinetic energy components reveal that the orbitals involved in the covalent binding are σ_{2p} AO of B and 2S and σ_{2p} AO of N and C atoms in H_3B–NH_3 and H_3B–CO respectively.

Keywords. ZDO; deorthogonalization; one-particle density; interference density; kinetic interference energy; ammonia-borane; carbonyl-borane.

1. Introduction

According to the conventional concept of chemists, ammonia borane (or borazane), H_3B–NH_3, and carbonyl borane, H_3B–CO, are formed by the sharing of a lone pair of electrons belonging to the donor groups (NH_3, CO) with the vacant orbital of the acceptor group (BH_3). The newly formed B–*L* bond (*L* is any ligand) is of pivotal importance to account for the stability and characteristics of such boron coordination compounds. A number of theoretical calculations probing the various aspects of these two molecules have appeared (Das 1957; Hoffmann 1964; Veillard *et al* 1967; Moireau and Veillard 1968; Peyerim Hoff and Buenker 1968; Armstrong and Perkins 1969; Lloyd and Lynaugh 1970, 1972; Frost 1970; Shillady *et al* 1971; Gordon and England 1972; Palke 1972; Bach *et al* 1973; Fujimoto *et al* 1974; Kato *et al* 1974; Purcell and Martin 1974; Runtz and Bader 1975; Dill *et al* 1975; Umeyama and Morokuma 1976; Ermler *et al* 1976; Ha 1976; Datta *et al* 1977; Redmon *et al* 1979; Zirz and Alrichs 1981).

The probing into the nature of the newly formed bond of these compounds has so far been in terms of Mulliken (1955) population analysis which can make only a qualitative prediction as to the distribution of electrons and the binding effect. Ruedenberg (1962) suggested an energy analysis, based on density matrix properties, which can extract significant energetic information that provides a quantitative basis of reasoning about the contributory factors to chemical binding. Ruedenberg concluded that the accumulation of a non-classical electron density called interference density, arising out of the interference of AO's on the atoms approaching to form covalent bond, is

responsible for the chemical binding through the lowering of non-classical electronic kinetic energy, known as kinetic energy due to interference. The concept was applied to a number of molecular system (Layton Jr and Ruedenberg 1964; Rue and Ruedenberg 1964; Edmiston and Ruedenberg 1964; Popkie and Moffatt 1968; Fienberg *et al* 1970). Wilson and Goddard (1970, 1972) critically analyzed the role of kinetic energy in covalent binding and concluded, from the analysis of GI functions of molecules, that lowering of a non-classical 'exchange kinetic energy' is responsible for chemical binding and this 'exchange kinetic energy' is related to the interference kinetic energy of Ruedenberg. Recently, a number of reports have appeared on the calculation of interference density and the kinetic interference energy (Datta 1976; Datta and Datta 1978), but some fundamental discrepancies are evident in this work (vide infra).

The purpose of the present investigation is to extract information as to whether Ruedenberg's type of binding analysis can be attempted by semi-empirical ZDO methods like CNDO/2 (Pople *et al* 1965). The CNDO/2 method, inspite of its success in correlating a number of molecular properties with experimental results (Pople and Gordon 1967) and its easy applicability to large molecules, especially, the boron coordination compounds (Labarre 1978), calculates unrealistic charge distribution (Shillady *et al* 1971) because, the basis functions of this formalism are virtually a set of orthogonalized AO's (Pople and Segal 1965).

The spinles one-particle (electron) density $\rho(R)$ at a position R for a closed shell molecular system expanded in terms of AO's takes the form

$$\rho(R) = \sum_{r,s} P(r,s)\phi_r(R)\phi_s(R), \tag{1}$$

where $P(r, s)$ are the elements of bond order matrix and ϕ_i's are the basis set. Integration of $\rho(R)$, over all space, for methods that include overlap, gives the population breakdown

$$N = \int \rho(R)\,\mathrm{d}R = \sum_{r,s} P(r,s)\,S(r,s) \tag{2}$$

$$= \sum_{A}^{\text{atoms}} P_A^N + \sum_{A}^{\text{atoms}} \sum_{B>A}^{\text{atoms}} P_{AB}, \tag{3}$$

where N is the total number of electrons and $S(r, s)$ is the overlap integral between AO's r and s, and P_A^N and P_{AB} are the net atomic and overlap populations respectively,

$$P_A^N = \sum_{r}^{A}\sum_{s}^{A} P(r,s)\,S(r,s), \tag{4}$$

$$P_{AB} = 2\sum_{r}^{A}\sum_{s}^{B} P(r,s)\,S(r,s), \tag{5}$$

but for ZDO methods, (2) takes the form

$$N = \sum_{A}^{\text{atoms}}\sum_{r}^{A} P(r,r). \tag{6}$$

Ruedenberg suggested a partitioning of the electron density $\rho(R)$ into the quasi-classical density $\rho^{\text{cl}}(R)$, and interference density $\rho^{I}(R)$

$$\rho(R) = \rho^{\text{cl}}(R) + \rho^{I}(R), \tag{7}$$

with the conservation relation

$$N = \int \rho(R)\,dR = \int \rho^{cl}(R)\,dR, \tag{8}$$

and

$$\int \rho^{I}(R)\,dR = 0. \tag{9}$$

Imposing the conditions (8) and (9), and applying the series of approximation regarding the interacting orbital pair (Ruedenberg 1962; Edmiston and Ruedenberg 1964) the formula of interference density has been derived as

$$\rho^{I} = \sum_{Aa,Bb} \rho^{I}(Aa\,Bb) = \sum_{Aa,Bb} P(Aa\,Bb) \langle Aa\,Bb \rangle, \tag{10}$$

where Aa, Bb are AO's centred on atoms A and B respectively, $P(Aa\,Bb)$ is the element of bond order matrix and $\langle Aa\,Bb \rangle$ is the orbital interference density for the orbital pair (Aa, Bb)

$$\langle Aa\,Bb \rangle = Aa \cdot Bb - \tfrac{1}{2} S(Aa\,Bb)(Aa^2 + Bb^2), \tag{11}$$

where $S(Aa\,Bb)$ is the overlap integral of the AO pair. To measure the degree to which an orbital (Aa) is effective in creating interference effect, Ruedenberg, similar to that of McWeeny (1951) and Mulliken (1955), partitioned the population $q(Aa)$ of the orbital into 'valence inactive', $P(Aa)$, and 'valence active', $v(Aa)$, parts.

$$q(Aa) = P(Aa) + v(Aa), \tag{12}$$

where,

$$P(Aa) = P(Aa\,Aa), \tag{13}$$

and

$$v(Aa) = \sum_{Bb} P(Aa\,Bb) S(Aa\,Bb). \tag{14}$$

The relative size and sign of $v(Aa)$ determines the binding capacity of the orbital (Aa).

Now under a ZDO formalism, the overlap distribution $(Aa \cdot Bb)$ and the overlap integral $S(Aa\,Bb)$ are all zero thereby excluding any possibility of inclusion of interference effect in CNDO/2 method, and the electron density is given by the quasi-classical density only and the valence activity (equation (14)) is zero. For the same reason, overlap population, although used as bond index (Fischer and Kollmar 1970; Ehrenson and Seltzer 1971; Corre 1981), cannot be extracted from a CNDO/2 calculation where the total charge density is divided out formally among the atoms alone (equation 6), and under such a formalism, the identification of bond is not straight forward (McIver *et al* 1971; Driessler and Kutzelnigg 1977).

Thus it is apparent that the CNDO/2 method is not at all suitable for the analysis of molecular binding whatsoever, and the fundamental discrepancies apparent in Datta (1976), and Datta and Datta (1978) may now be mentioned (i) these authors have calculated interference density and related properties through the localized molecular orbitals. But it is not *a priori* clear how the interference effect which arises due to the wave-like behaviour of fundamental particles (Ruedenberg 1962) is incorporated in a localized orbital framework. However, Nakatsuji (1974) showed how interference effect can be included in localized orbitals and this seems to have been overlooked by Datta and Datta (ii) Datta (1976), in his study of the interference effect in LiH system,

claims to use the available localized orbitals of Edmiston and Ruedenberg (1965) obtained from the delocalized set of Ransil (1960). On the other hand, Layton Jr and Ruedenberg (1964) studied the chemical binding in the same system by the same method using the same wave function of Ransil. But it is apparent that the corresponding values of Datta are different from that of Layton Jr and Ruedenberg, and the same wavefunction (evaluated at the equilibrium distance) has been used over a range of 21 distances of internuclear separation—the reason for which are not mentioned in the paper (iii) Datta and Datta (1978) have calculated interference density at the bonding region through CNDO/2 functions. But interference effect cannot arise here because of the orthogonal nature of the basis functions, which cannot be changed by the unitary transformation converting the delocalized set into a localized one. Thus, the work is not consistent with the basic philosophy of CNDO/2 formalism.

However, Shillady *et al* (1971) noted that a CNDO/2*D* formalism, in which the orbitals from the CNDO/2 calculations are deorthogonalized by Löwdin (1950) transformation, gives charge distribution that follows closely the trend of *ab initio* calculations, and McIver *et al* (1971) noted that the charge density distribution found by such a method is comparable with experimental results. Since the basis set is not orthogonal, the overlap distribution $(Aa \cdot Bb)$ and the overlap integral $S(Aa\,Bb)$ are no longer zero and the inclusion of interference effect is theoretically justified in CNDO/2*D* formalism. We have therefore, undertaken a CNDO/2*D* study of charge distribution, in terms of orbital and overlap population, in H_3B–NH_3 and H_3B–CO as compared to the available *ab initio* results. We have also computed one-particle density, interference density at the bond mid-point and the kinetic part of the interference energy, the bond population as functions of internuclear separation between the donor and the acceptor to study the variation of covalent binding with internuclear distance by the same method. The two-centre energy term, E_{A-B}, and one of its components for the new bond are computed, to use as bond index, by CNDO/2 energy partitioning.

2. Method of computation

The geometric parameters of the donors, the acceptor and the adducts are optimized by CNDO/2 method using standard parameters and STO basis set. The overlap and coulomb integrals are evaluated from the explicit expressions derived by Roothaan (1951). The B-L bond is made to coincide with $Z(C_3)$ axis of the coordinate system. The CNDO/2 density matrix is deorthogonalized according to Löwdin's prescription (Löwdin 1950)

$$\mathbf{P}' = \mathbf{S}^{-1/2}\mathbf{P}\mathbf{S}^{-1/2} \tag{15}$$

where $\mathbf{P}$ and $\mathbf{P}'$ are the density matrices corresponding to orthogonal and non-orthogonal bases, and $\mathbf{S}$ is the overlap matrix over Slater orbitals respectively. $\mathbf{P}'$ is used to calculate charge distribution through equations (4) and (5). The computed orbital populations, and CNDO/2 vis-a-vis CNDO/2*D* charge distribution of all the chemical species at CNDO/2 equilibrium geometry are shown in table 1 and figure 1 respectively. The orbital pairwise decomposed B–N, B–C and C–O bond populations are shown in tables 2–4 respectively. The acceptor and the donor moieties are kept at geometry to which they are reorganized in the adducts and a series of wavefunctions are calculated as functions of B–N and B–C bond lengths and the corresponding CNDO/2 density matrices are deorthogonalized (equation 15) and used to calculate $\mathbf{P}_{AB}$, ρ and ρ' at the

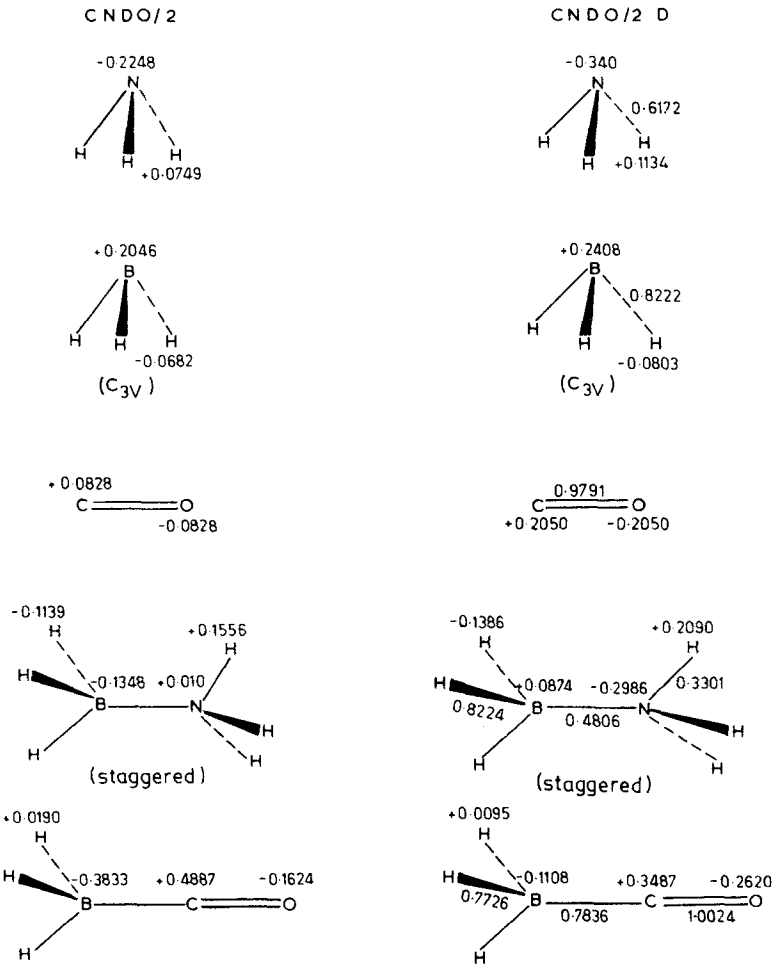

Figure 1. Charge distribution in the donors, the acceptor and the adduct.

bond mid-point, and T^I, the kinetic part of the interference energy, is calculated by the formula

$$T^I = \int \hat{T}\rho^I(R)\,\mathrm{d}R$$

$$= \sum_{Aa}\sum_{Bb} P(Aa\,Bb)\int \hat{T}\langle Aa\,Bb\rangle\,\mathrm{d}R$$

$$= \sum_{Aa}\sum_{Bb} P(Aa\,Bb)T\langle Aa\,Bb\rangle, \tag{16}$$

where $\hat{T}$ is the operator for kinetic energy and the integral $T\langle Aa\,Bb\rangle$ is the kinetic energy of the orbital interference density (equation (11)).

$$T\langle Aa\,Bb\rangle = [T(Aa\,Bb) - \tfrac{1}{2}S(Aa\,Bb)\{T(Aa\,Aa)+T(Bb\,Bb)\}], \tag{17}$$

Table 1. Gross population analysis for the donors, the acceptor and the adducts.

AO	Donors and Acceptors	Adducts	
	$BH_3(C_{3v})$	BH_3–NH_3	BH_3–CO
B_{2s}	1·0488	0·9361	0·9144
B_{2p_x}, B_{2p_y}	0·8272	0·7771	0·8143
B_{2p_z}	0·0560	0·4222	0·5680
H_{1s}(B)	1·0803	1·1386	0·9905
	NH_3		
N_{2s}	1·6311	1·5057	
N_{2p_x}, N_{2p_y}	1·0244	1·1170	
N_{2p_z}	1·6600	1·5588	
H_{1s}(N)	0·8866	0·7910	
	CO		
C_{2s}	1·7416		1·3980
C_{2p_x}, C_{2p_y}	0·5453		0·6435
C_{2p_z}	0·9627		0·9664
O_{2s}	1·8633		1·8585
O_{2p_x}, O_{2p_y}	1·4547		1·5350
O_{2p_z}	1·4322		1·3336

Table 2. Breakdown of the B–N bond population (BH_3–NH_3).

Orbital pairs	Populations
B_{2s}/N_{2s}	−0·0125
B_{2s}/N_{2p_z}	0·0658
B_{2p_z}/N_{2s}	0·1925
B_{2p_z}/N_{2p_z}	0·2050
$\pi(B_{2p_x}/N_{2p^x})$	0·0150
$\pi(B_{2p_y}/N_{2p_y})$	0·0150

Table 3. Breakdown of the B–C bond population (BH_3–CO).

Orbital pairs	Populations
B_{2s}/C_{2s}	−0·0077
B_{2s}/C_{2p_z}	0·0556
B_{2p_z}/C_{2s}	0·3426
B_{2p_z}/C_{2p_z}	0·1677
$\pi(B_{2p_x}/C_{2p_x})$	0·1127
$\pi(B_{2p_y}/C_{2p_y})$	0·1127

where the matrix elements are given by

$$T(Aa\,Bb) = \int Aa(R)\hat{T}\,Bb(R)\,\mathrm{d}R, \tag{18}$$

$$T(Aa\,Aa) = \int Aa(R)\hat{T}\,Aa(R)\,\mathrm{d}R, \tag{19}$$

Table 4. Breakdowns of the populations for the C–O bond in free CO as well as in H_3B–CO.

Orbital pairs	Populations	
	(a)	(b)
C_{2s}/O_{2s}	−0·2110	−0·0992
C_{2s}/O_{2p_z}	0·0753	0·2267
C_{2p_z}/O_{2s}	0·0706	−0·0464
C_{2p_z}/O_{2p_z}	0·4221	0·3804
$\pi(C_{2p_x}/O_{2p_x})$	0·3110	0·2704
$\pi(C_{2p_y}/O_{2p_y})$	0·3110	0·2704

(a) Free CO at the same geometry as in H_3B–CO; (b) CO moiety in H_3B–CO.

$$T(Bb\,Bb) = \int Bb(R)\hat{T}\,Bb(R)\,\mathrm{d}R. \tag{20}$$

The $T(Aa\,Bb)$ elements are computed through the explicit formulae of Roothaan (1951). In computing ρ the entire basis set is included, but in computing ρ^I the principal interacting orbitals of B, N and C only are considered. The two-centre energy terms E_{A-B} for bonded interaction are a measure of the strength of chemical bond and have five components (Fischer and Kollmar 1970)

$$E_{AB} = E^R_{AB} + E^V_{AB} + E^J_{AB} + E^K_{AB} + E^N_{AB}, \tag{21}$$

of which E^R_{AB}, the contribution of resonance integrals to the energy of the A–B bond, is the main feature of the covalent bond and closely correlates with the E_{AB} values. The E_{AB} and its E^R_{AB} components are computed for each B–N and B–C separation. The computed values of ρ, ρ^I, T^I, E_{AB}, E^R_{AB} and P_{AB} are shown in tables 5 and 6 for H_3B–NH_3 and H_3B–CO respectively. The orbital pairwise decomposition of ρ^I and the corresponding T^I are shown in tables 7 and 8 for B–N and B–C bonds respectively.

Table 5. $\rho(R)$, $\rho^I(R)$, T^I, E_{A-B}, E^R_{A-B}, and the bond populations at several distances of B–N separation in borazane.

r(B–N), (Å)	$\rho(R)$	$\rho^I(R)$	T^I (a.u.)	E_{A-B} (a.u.)	E^R_{A-B} (a.u.)	B–N bond population
1·165	0·4237	0·0654	−0·0049	−0·7657	−1·4412	0·4222
1·365	0·2837	0·0537	−0·1690	−0·8719	−1·1619	0·4976
1·565	0·1885	0·0419	−0·2603	−0·8119	−0·9133	0·4806
1·765	0·1228	0·0311	−0·2913	−0·6765	−0·6914	0·4189
1·965	0·0771	0·0216	−0·2744	−0·5172	−0·4984	0·3355
2.165	0·0461	0·0140	−0·2281	−0·3196	−0·2921	0·2482
3·50	0·0426	0·0001	−0·0068	−0·0136	−0·0060	0·0051

(R) = mid point of r(B–N).

Table 6. The $\rho(R)$, $\rho^I(R)$, T^I, E_{A-B}, E^R_{A-B} and B–C bond populations at several distances of B–C separation in carbonyl borane.

r(B–C) (Å)	$\rho(R)$	$\rho^I(R)$	T^I (a.u.)	E_{A-B} (a.u.)	E^R_{A-B} (a.u.)	*B–C* bond populations
1·04	0·3558	0·0810	0·1031	−1.2171	−2.0305	0·8202
1·24	0·2692	0·0579	−0·0416	−1·3772	−1·6987	0·8705
1·44	0·1998	0·0432	−0·1434	−1·2932	−1·3804	0·7836
1·64	0·1456	0·0320	−0·1962	−1·0890	−1·0785	0·6418
1·84	0·1033	0·0237	−0·2122	−0·8492	−0·8080	0·5030
2·04	0·0714	0·0170	−0·2002	−0·6231	−0·5807	0·3797
3·50	0·0023	0·0003	−0·0101	−0·0134	−0·0137	0·0102

R = mid point of r(*B–C*).

Table 7. The orbital pair-wise breakdowns of the interference density and the corresponding interference kinetic energies at several distances of B–N separation in borazane.

r (B–N), (Å)	$\rho^I_{2s/2s}(R)$	$\rho^I_{2s/2p}(R)$	$\rho^I_{2p/2s}(R)$	$\rho^I_{2p/2p}(R)$	$T^I_{2s/2s}$	$T^I_{2s/2p}$	$T^I_{2p/2s}$	$T^I_{2p/2p}$
1·165	−0·0055	0·0036	0·0110	0·0563	0·0417	−0·0208	−0·0576	0·0318
1·365	−0·0022	0·0061	0·0096	0·0403	0·0178	−0·0442	−0·0779	−0·0646
1·565	−0·0005	0·0057	0·0078	0·0289	0·0046	−0·0509	−0·0862	−0·1278
1·765	0·0002	0·0045	0·0061	0·0203	−0·0019	−0·0498	−0·0841	−0·1556
1·965	0·0004	0·0032	0·0044	0·0137	−0·0045	−0·0429	−0·0745	−0·1525
2·165	0·0003	0·0021	0·0030	0·0086	−0·0051	−0·0338	−0·0598	−0·1294
3.50	0	0·00002	0·00003	0·00007	−0·0002	−0·0009	−0·0017	−0·0040

(R) = mid point of r(B–N).

Table 8. The orbital pair-wise breakdowns of the interference density and the corresponding interference kinetic energies at several distance of B–C separation in carbonyl borane.

r(B–C), (Å)	$\rho^I_{2s/2s}(R)$	$\rho^I_{2s/2p}(R)$	$\rho^I_{2p/2s}(R)$	$\rho^I_{2p/2p}(R)$	$T^I_{2s/2s}$	$T^I_{2s/2p}$	$T^I_{2p/2s}$	$T^I_{2p/2p}$
1·04	−0·0052	0·0039	0·0198	0·0625	0·0388	−0·0171	−0·0552	0·1366
1·24	−0·0018	0·0034	0·0155	0·0408	0·0133	−0·0201	−0·0815	0·0468
1·44	−0·0002	0·0032	0·0127	0·0274	0·0017	−0·0245	−0·0990	−0·0216
1·64	0·0004	0·0026	0·0104	0·0186	−0·0032	−0·0243	−0·1055	−0·0633
1·84	0·0005	0·0021	0·0082	0·0128	−0·0055	−0·0231	−0·1018	−0·0817
2·04	0·0006	0·0017	0·0062	0·0087	−0·0065	−0·0203	−0·0904	−0·0831
3·50	0·00002	0·00003	0·0001	0·0001	−0·0005	−0·0009	−0·0040	−0·0047

(R) = mid point of r(B–C).

3. Results and discussion

The HB̂H angle reorganizes to 110° in both the complexes. The B–H bond length is 1·19 Å and remains unchanged. The planar (D_{3h}) to pyramidal (C_{3v}) reorganization energy of BH_3 is 0·0359 a.u. (22·57 kcal/mol) which is in good agreement with the values

obtained by several non-empirical methods (Armstrong and Perkins 1969; Ermler *et al* 1976; Umeyama and Morokoma 1976). The HN̂H angle changes from 105° to 109·25°, and the N–H bond length (1·07 Å) remains unchanged, on adduct formation. The reorganization energy of NH_3 is negligible (0·0019 a.u). The optimized B–N bond length 1·565 Å, is in very good agreement with its experimental value 1·56 Å (Shore and Parry 1955; Hughes 1956; Lippert and Lipscomb 1956). The optimized B–C bond length is 1·44 Å which is also in good agreement with its experimental value (Herzberg 1966). The C–O bond stretches from 1·19 to 1·211 Å and the reorganization energy of CO is negligible (0·0019 a.u). The staggered form of borazane is the stabler one.

3.1 *Mulliken population analysis*

3.1a *Ammonia borane*: From figure 1 we see that the CNDO/2*D* formal charges on B in $BH_3(C_{3v})$ is positive and that on N in NH_3 is negative and these formal charges do not change appreciably on molecular formation although, 0·3284 a.u of charge has been formally transferred from the donor to the acceptor. But the formal charges on all the H atoms changes significantly on adduct formation. The charge density on H attached to B changes from $-0{\cdot}0803$ a.u to $-0{\cdot}1386$ a.u and that on H attached to N changes from $+0{\cdot}1134$ a.u to $+0{\cdot}2090$ a.u. Since B is nearly neutral and N is strongly negative in the complex, the charge rearrangement contradicts the classical belief of the formation of the dative bond by the donation of lone pair of electron of N to the empty orbital of B. From table 1 we see that the population in B_{2p_z} orbital increases considerably and those in all the other B orbital decreases, while in N, the charge donating atom, the populations in $2s$ and $2p_z$ orbitals decrease and those in $2p_x$ and $2p_y$ orbitals increases. The overlap population of the B–N bond is surprisingly low compared to those of B–H and N–H bonds. Table 2 demonstrates that the B_{2s}/N_{2s} overlap population is a negative number (antibonding) and the B–N bond is essentially constructed from $2p_\sigma$ orbital of B and $2s$ and $2p_\sigma$ orbitals of N, and the major contributors are the $2p_\sigma$ orbital pair. Thus the charge transfer originates mostly from the N_{2p_z} orbital to the B_{2p_z} orbital and a charge readjustment finally takes place between the two central atoms and the H atoms bound to them to make N atom strongly negative and B atom virtually uncharged. This same pattern of charge distribution and bond formation in this molecule were found by several *ab initio* calculations (Veillard *et al* 1967; Moireau and Veillard 1968; Armstrong and Perkins 1969). On the other hand, CNDO/2 method overestimates the net transfer of charge (0·4765 a.u) and gives positive charge on N and negative charge on B (figure 1), which was also noted by Shillady *et al* (1971). Moreover, the bond formation cannot be studied by CNDO/2 method.

3.1b *Carbonyl borane*: Figure 1 demonstrates that the formal charges on C of CO and B of BH_3 are positive. Thus the formation of BH_3–CO involves the joining of two positively charged fragments. The net balance of charge transfer is 0·08 a.u. of electronic charge from CO moiety to the BH_3 moiety. These two facts suggest that, during the process of bond formation, both the interacting groups act in a concerted way to donate and accept charge. On adduct formation, the B atoms are formally negatively charged while the H atoms are positively charged, and the formal positive charge on C and negative charge on O are increased. Table 1 demonstrates that the population in $B(2p_z)$ orbital increases considerably while those in other B orbitals decrease to some extent, and of the orbitals of C, the population in $2s$ decreases while those in other orbitals increase; of the oxygen orbitals, the populations in $2s$ and $2p_z$ orbitals decrease and

those in $2p_x$, $2p_y$ orbitals increase. From table 3 we see that the B_{2s}/C_{2s} overlap population is antibonding and the binding effect comes through the $2p_\sigma$ orbital of B and $2s$ and $2p_\sigma$ orbital of C. Thus the charge donation stems from the $2s$ and $2p_z$ orbitals of C into the $2p_z$ orbital of B and as a final adjustment charge migrates from O($2s$) and O($2p_z$) orbitals into C($2s$) and C($2p_z$) orbitals. The amount of charge migrated from B($2s$) orbital must be donated to the H atoms. Since the magnitude of π(B–C) population is considerable and the electron density around H atoms is decreased, the back-donation of charge from BH_3 to CO must be taking place through the 'hyperconjugative' mechanism as suggested by Graham and Stone (1956). The pi-orbitals of B, C and O atoms have simultaneous overlap with the group orbitals of three H atoms to drift charge around H towards C and O. Thus Mulliken's categorisation of CO as an 'amphodonor' is also supported by this CNDO/2-*D* calculation.

One more interesting point to note is the dramatic increase in C–O bond population on adduct formation (figure 1), which may be offered as a natural explanation of the spectroscopic observation of the increase in CO stretching frequency on complex formation with BH_3 (Bethke and Wilson 1957; Taylor 1957; Sundaram and Cleveland 1960; Cowan 1949, 1950). The breakdowns of the bond populations of the free CO at the same geometry as in the complex, and of CO in the complex into orbital pairwise components (table 4) show that the observed increase in the C–O bond population arises from the reduction of the large antibonding C_{2s}/O_{2s} population and from an increase of C_{2s}/O_{2p_z} population on complex formation. This pattern of charge redistribution within the donor and the acceptor and the mechanism of bond formation were also observed by several *ab initio* calculations (Armstrong and Perkins 1969; Runtz and Bader 1975; Kato *et al* 1974; Ermler *et al* 1976; Umeyama and Morokuma 1976). Although the gross patterns of charge rearrangement are the same in both CNDO/2 and CNDO/2-*D* methods, the former over-estimates the net transfer of charge (figure 1).

3.2 *The one-particle density, the interference density and the kinetic interference energy, and other bond indices.*

The quantities in tables 5 and 6 have a common trend of variation. The binding interaction starts at a sufficiently large R, the distance of internuclear separation between the atoms forming the new bond. The bond-populations, one-particle density and the interference density at the bond mid-point steadily grow as R decreases, indicating a piling of charge density in the bonding region in both the systems. The E^R_{AB}, the resonance integral, steadily decreases with decrease of R, while E_{AB}, the energy of the newly formed bond, closely correlates with the A–B bond-population and passes through a minima at shorter R where the latter is maximum. It is further noted that the sum of the reorganization energies of the donor and the acceptor is over-compensated by the energies of the newly formed bond in both the systems over a considerably large range of internuclear separation.

The kinetic interference energy T^I starts with a negative value at large R and sharply decreases with the decrease in R, and then rapidly increases below R_e, the equilibrium R, for both the systems under study. However, T^I remains negative over the entire range of study in H_3B–NH_3, and becomes positive at shorter R values below R_e in H_3B–CO. The plot of T^I values as functions of R (figure 2) shows that the kinetic interference energy passes through a minimum near but above R_e, and the curve conforms to the

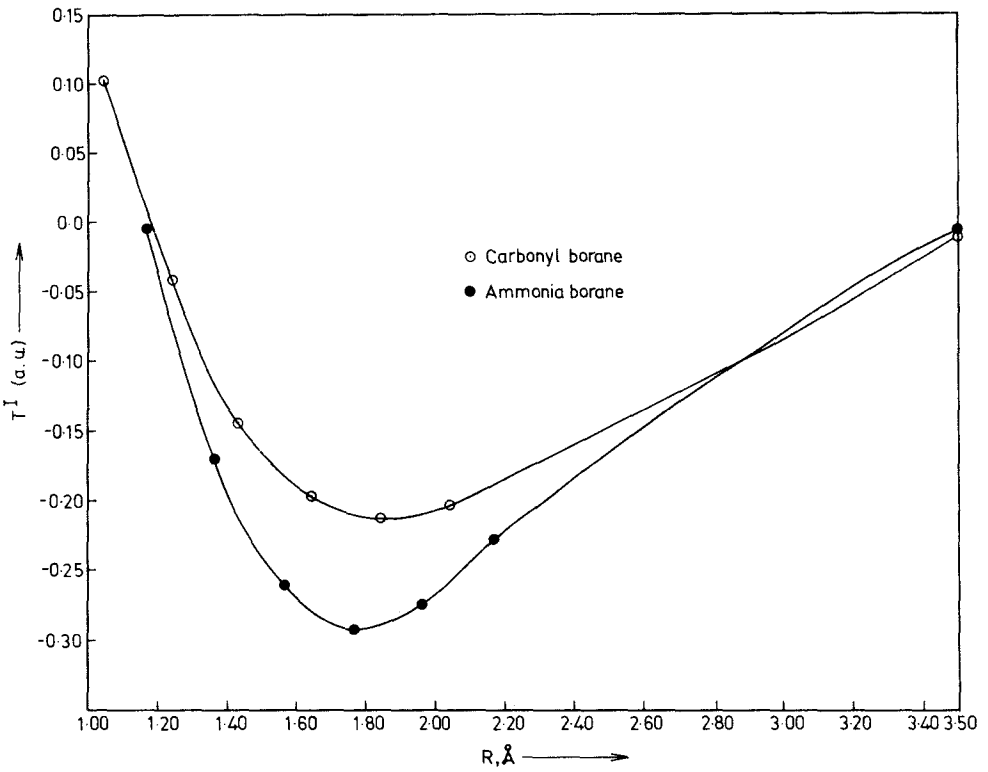

Figure 2. Plot of the kinetic interference energy as a function of internuclear distance.

general pattern of the kinetic component of Morse curve (Slater 1933; Eyring *et al* 1944). According to the kinetic component of the Morse curve, kinetic energy decreases as R decrease and then increases rapidly as the nuclei are brought closer together. Ruedenberg (1962) argued that such lowering of kinetic energy comes through interatomic interference, and he conjectured that due to cluster promotion atoms form the promotion states in which potential energy is decreased and kinetic energy is excessively increased leading to an overall promotion, and subsequent interference causes a large compensating lowering in kinetic energy. At larger R, cluster promotion is less important and pure interference effect is possible to lower the kinetic energy, but at shorter R, particularly at and around R_e, cluster promotion is important and therefore kinetic energy should start increasing. Although there is no scope of inclusion of cluster promotion in the present calculation, the general trend of variation of T^I values with R is consistent with the experimental curve of variation in kinetic energy as function of internuclear separation (the kinetic component of Morse curve).

The interference density of $2s$(B)/$2s$(N) orbital pair is positive (bonding) at larger R values and negative (antibonding) at and below R_e (table 7). The corresponding kinetic energy component $T^I_{2s/2s}$ is consistent with the nature of interference, negative at larger R values and positive at shorter R values. This orbital pair, therefore, has a binding effect at longer distances and antibinding effect at shorter distances of approach. We also noted the antibonding contribution of this orbital pair towards the B–N bond

population (table 2). The interference densities due to all the other orbital pairs are positive and increase steadily with decrease of R and the major part of the interference density is constructed by $2p/2p$ orbital pair followed by that of B($2p$)/N($2s$) pair at all R. The corresponding kinetic energy components reveal that the interference interaction due to all these orbital pairs starts with a binding effect from a large R and grow steadily with decreasing R, and then increases at further closer approaches. The $T^I_{2s/2p}$ and $T^I_{2p/2s}$ components pass through a minima at R_e while the minima of the $T^I_{2p/2p}$ component is above R_e, and increases very sharply at shorter R values indicating a stronger localisation of electron near the nuclei. However, starting from large R up to R_e the major fraction of the interference energy is contributed by the $2p/2p$ orbital pair followed by that of B($2p$)/N($2s$) orbital pair, signifying that the B–N bond is principally formed due to electron sharing by $2p_\sigma$ orbital of B with $2s$ and $2p_\sigma$ orbitals of N.

Table 8 demonstrates that B($2s$)/C($2s$) orbital pair creates a constructive interference at longer R and a destructive interference at and below R_e. The antibonding effect of this orbital pair is also noted in population analysis (table 3). The corresponding kinetic energy component $T^I_{2s/2s}$ is consistent with the nature of interference *i.e.* it is negative at larger values and positive at and below R_e. The interference densities due to other orbital pairs increase monotonically with decrease in R and $2p$ orbitals, followed by B($2p$)/C($2s$) pair, construct the major fraction of interference density. The corresponding kinetic energy components, however, behave dissimilarly with those of borazane system. The $T^I_{2s/2p}$ and $T^I_{2p/2s}$ components decrease first, pass through minima, then increase with the decrease of R. The $T^I_{2p/2s}$ and $T^I_{2p/2p}$ components decrease hand in hand at larger R values, but at shorter R values the latter increases very sharply and becomes positive. The sharper increase in the kinetic energy components of $2p$ orbital pair in this system may be due to the much closer approach of the interacting groups. Thus, the B–C bond is principally formed by $2_{p\sigma}$ orbital of B, and $2s$ and $2_{p\sigma}$ orbital of C.

One more point to be discussed is the kinetic energy components of $2p$ orbital pairs below R_e. These quantities are positive at shorter distances below R_e in spite of the positive interference density of these orbital pairs (tables 7, 8). A closer look at the definition of kinetic interference energy (equations (16) and (17)) shows that the sign of this quantity depends on the signs of the element of bond order matrix and the integral $T\langle Aa\,Bb\rangle$. The latter and not the former, should be very sensitive of R. Although the atomic quantities $T(Aa\,Aa)$ and $T(Bb\,Bb)$ remain constant at all R because of non-inclusion of cluster promotion in the present calculation, $T(Aa\,Bb)$ and $S(Aa\,Bb)$ change with R to reverse the sign of the integral $T\langle Aa\,Bb\rangle$ at shorter distances below R_e.

4. Conclusion

Thus we see that CNDO/2D calculation has reproduced the trend of charge distribution, in terms of orbital and overlap populations, of the *ab initio* method in H_3B–NH_3 and H_3B–CO fairly well. The CNDO/2 bond indices E_{AB} and E^R_{AB}, and CNDO/2-D derived quantities like P_{AB}, ρ, ρ^I and T^I all indicate the binding situation as functions of internuclear separation. E_{AB} and E^R_{AB} are semi-empirical quantities while ρ is a very useful tool for studying various chemical phenomena (McWeeny 1954; Bamzai and Deb 1981) and ρ^I is a fundamental quantity for covalent binding. The variation of T^I with R conforms to the kinetic component of the Morse curve. Thus one can say that

the numerical results obtained were consistent with the concepts associated with the theoretical quantities. The CNDO/2-*D* method, therefore, appears to be a good approach to extract useful information on chemical binding.

References

Ahlrichs R and Koch W 1978 *Chem. Phys. Lett.* **53** 341
Armstrong D R and Perkins P G 1969 *J. Chem. Soc.* (A) 1044
Bach M C, Crasnier F, Labarre J F and Leibovici C 1973 *J. Mol. Struct.* **16** 89
Bamzai A S and Deb B M 1981 *Rev. Mod. Phys.* **53** 95
Bethke G W and Wilson M K 1957 *J. Chem. Phys.* **26** 1118
Corre F 1981 *J. Mol. Struct.* **86** 69
Cowan R D 1949 *J. Chem. Phys.* **17** 218
Cowan R D 1950 *J. Chem. Phys.* **18** 1101
Das T P 1957 *J. Chem. Phys.* **27** 1
Datta R 1976 *Indian J. Chem.* **A14** 269
Datta R and Datta M K 1978 *Natl. Acad. Sci. Lett.* **1** 101
Datta R and Datta M K 1978 *Indian J. Chem.* **A16** 616
Datta R, Datta M K and Ghosh D C 1977 *Indian J. Chem.* **15** 259
Dill J D, Schleyer P V R and Pople J A 1975 *J. Am. Chem. Soc.* **97** 3402
Drissler F and Kutzelnigg W 1977 *Theor. Chim. Acta* **43** 307
Edmiston C and Ruedenberg K 1964 *J. Phys. Chem.* **68** 1628
Edmiston C and Ruedenberg K 1965 *J. Chem. Phys.* **43** S97
Ehrenson S and Seltzer S 1971 *Theor. Chim. Acta* **20** 17
Ermler W C, Glasser F D and Kern C W 1976 *J. Am. Chem. Soc.* **98** 3799
Eyring H, Walter J and Kimball G 1944 Quantum chemistry (New York: John Wiley)
Feinberg M J, Ruedenberg K and Mehler E L 1970 *Adv. Quantum Chem.* **5** 27
Fischer H and Kollmar H 1970 *Theor. Chim. Acta.* **16** 163
Frost A A 1970 *Theor. Chim. Acta* **18** 156
Fujimoto H, Kato S, Yamabe S and Fukui K 1974 *J. Chem. Phys.* **80** 572
Gordon M S and England W 1972 *Chem. Phys. Lett* **15** 59
Graham W A G and Stone F G A 1956 *J. Inorg. Nuclear Chem.* **3** 164
Ha T K 1976 *J. Mol. Struct.* **30** 103
Herzberg G 1966 *Electronic spectra of polyatomic molecules* (New York: Van Nostrand Reinhold)
Hoffman R 1964 *J. Chem. Phys.* **40** 2474
Hughes E W 1956 *J. Am. Chem. Soc.* **78** 502
Kato S, Fujimoto H, Yamabe S and Fukui K 1974 *J. Am. Chem. Soc.* **96** 2024
Labarre J F 1978 *Struct. Bonding* (Berlin) **35** 1
Layton Jr. E M and Ruedenberg K 1964 *J. Phys. Chem.* **68** 1654
Lippert E L and Lipscomb W N 1956 *J. Am. Chem. Soc.* **78** 503
Lloyd D R and Lynaugh N 1970 *Chem. Commun.* 1545
Lloyd D R and Lynaugh N 1972 *J. Chem. Soc.* **68** 947
Löwdin P O 1950 *J. Chem. Phys.* **18** 365
Mclver Jr J W, Coppens P and Nowak D 1971 *Chem. Phys. Lett.* **11** 82
McWeeny R 1951 *J. Chem. Phys.* **19** 1614
McWeeny R 1954 *Proc. R. Soc.* **A223** 63
Moireau M Cl and Veillard A 1968 *Theor. Chim. Acta* **11** 344
Mulliken R S 1955 *J. Chem. Phys.* **23** 1833
Nakatsuji H 1974 *J. Am. Chem. Soc.* **96** 24, 30
Palke W E 1972 *J. Chem. Phys.* **56** 5308
Peyerim Hoff S D and Buenker R J 1968 *J. Chem. Phys.* **49** 312
Popkie H E and Moffatt J B 1968 *Int. J. Quantum Chem.* **2** 565
Pople J A and Gordon M 1967 *J. Am. Chem. Soc.* **89** 4253
Pople J A, Santry D P and Segal G A 1965 *J. Chem. Phys.* **43** S129
Pople J A and Segal G A 1965 *J. Chem. Phys.* **43** S136

Purcell K F and Martin R L 1974 *Theor. Chim. Acta* **35** 141
Ransil B J 1960 *Rev. Mod. Phys.* **32** 245
Redmon L T, Purvis III G D and Bartlett R J 1979 *J. Am. Chem. Soc.* **101** 2856
Roothaan C C J 1951 *J. Chem. Phys.* **19** 1455
Rue R R and Ruedenberg K 1964 *J. Phys. Chem.* **68** 1976
Ruedenberg K 1962 *Rev. Mod. Phys.* **34** 326
Runtz G R and Bader R F W 1975 *Mol. Phys.* **30** 129
Shillady D D, Billingsley II F P and Bloor J E 1971 *Theor. Chim. Acta* **21** 1
Shore S G and Parry R W 1955 *J. Am. Chem. Soc.* **77** 6084
Slater J C 1933 *J. Chem. Phys.* **1** 687
Sundaram S and Cleverland F F 1960 *J. Chem. Phys.* **32** 166
Taylor R C 1957 *J. Chem. Phys.* **28** 1131
Umeyama H and Morokuma K 1976 *J. Am. Chem. Soc.* **98** 7208
Veillard A, Levy B, Daudel R and Gallais F 1967 *Theor. Chim. Acta* **8** 312
Wilson Jr. C W and Goddard III W A 1970 *Chem. Phys. Lett.* **5** 45
Wilson Jr. C W and Goddard III W A 1972 *Theor. Chem. Acta* **26** 195
Zirz C and Ahlrichs 1981 *J. Chem. Phys.* **75** 4980